Pis'ma v ZhETF, vol. 102, iss. 9, pp. 688 – 694

Localization attractors in active quasiperiodic arrays

T. V. Laptyeva[+], *S. V. Denisov*[*×], *G. V. Osipov* [+], *M. V. Ivanchenko*[×1)]

[+] *Theory of Control and Dynamical Systems Department, Lobachevsky State University of Nizhny Novgorod, 603140 N. Novgorod, Russia*

[*] *Department of Theoretical Physics, University of Augsburg, 86159 Augsburg, Germany*

[×] *Department of Applied Mathematics, Lobachevsky State University of Nizhny Novgorod, 603140 N. Novgorod, Russia*

Submitted 3 September 2015

Resubmitted 16 September 2015

In dissipationless linear lattices, spatial disorder or quasiperiodic modulations in on-site potentials induce localization of the eigenstates and block the spreading of wave packets. Quasiperiodic inhomogeneities allow for the metal-insulator transition at a finite modulation amplitude already in one dimension. We go beyond the dissipationless limit and consider nonlinear quasi-periodic arrays that are additionally subjected to dissipative losses and energy pumping. We find finite excitation thresholds for oscillatory phases in both metallic and insulating regimes. In contrast to disordered arrays, the transition in the metallic and weakly insulating regimes display features of the second order phase transition accompanied by a large-scale cluster synchronization. In the limit of strong localization we find the existence of globally stable asymptotic states consisting of several localized modes. These localization attractors and chaotic synchronization effects can be potentially realized with polariton condensates lattices and cavity-QED arrays.

DOI: 10.7868/S0370274X15210079

Since the seminal paper of Anderson [1, 2], the phenomenon of eigenstate localization and absence of wave propagation in spatially modulated potentials remains in the focus of active studies for already fifty years. From the current perspective, the phenomenon can be obtained with spatial inhomogeneities of different types: an external dc field leads to Wannier–Stark localization and Bloch oscillations [3–5], random disorder yields Anderson localization [6], and quasiperiodic spatial modulations produce Aubry–Andre localization [7]. A fundamental nature of the localization phenomena has been experimentally demonstrated with electromagnetic [8], acoustic [9], and matter waves [10–13].

Effects of dissipation and energy gain in the systems exhibiting localization is currently receiving more and more attention, especially in the context of light propagation and lasing in active waveguide arrays [14–19], many-body quantum systems [20, 21], and exciton-polariton condensate arrays [22–25]. The key observation is that the localization is deteriorated under the action of dissipation/gain processes though it could survive weak non-Hamiltonian perturbations.

Effects of additional nonlinearity in dissipative disordered arrays have aslo been addresed. It was found that a dissipation introduced at the boundaries of a passive chain (or mimicked by semi-infinite propagating leads) leads to non-trivial changes in relaxation dynamics [26], transparency [27], and breaks the isotropy of wave propagation [28]. There are recent results for non-identical pairs and periodically inhomogeneous arrays that unveiled complex multi-stable and chaotic dynamics [29–32].

Recently we demonstrated that one-dimensional *active* disordered arrays can produce sparse oscillation patterns consisting of severeal Anderson modes, which we named *Anderson attractors* [33]. The Anderson model, however, has a feature: all its eigenstates become localized when an arbitrary small disorder is added to the array. Thus, the model does exhibit neither extended (metallic) inhomogeneous regimes nor transitions to localized (insulating) regimes when the disorder strength is varied. In this light the Aubry–Andre model with quasiperiodic potential deserves a particular attention [7, 34]. Its straightforward realization with spatially modulated optical potentials [34] has promoted ultracold atomic condensates as an accessible experimental testbed to explore the localization phenomena [11, 35–37]. A realization of spatially quasiperiodic exciton-polariton condensates has served another one [25].

In this paper we study localization effects in active quasiperiodic arrays within the framework of the dis-

[1)] e-mail: ivanchenko.mv@gmail.com

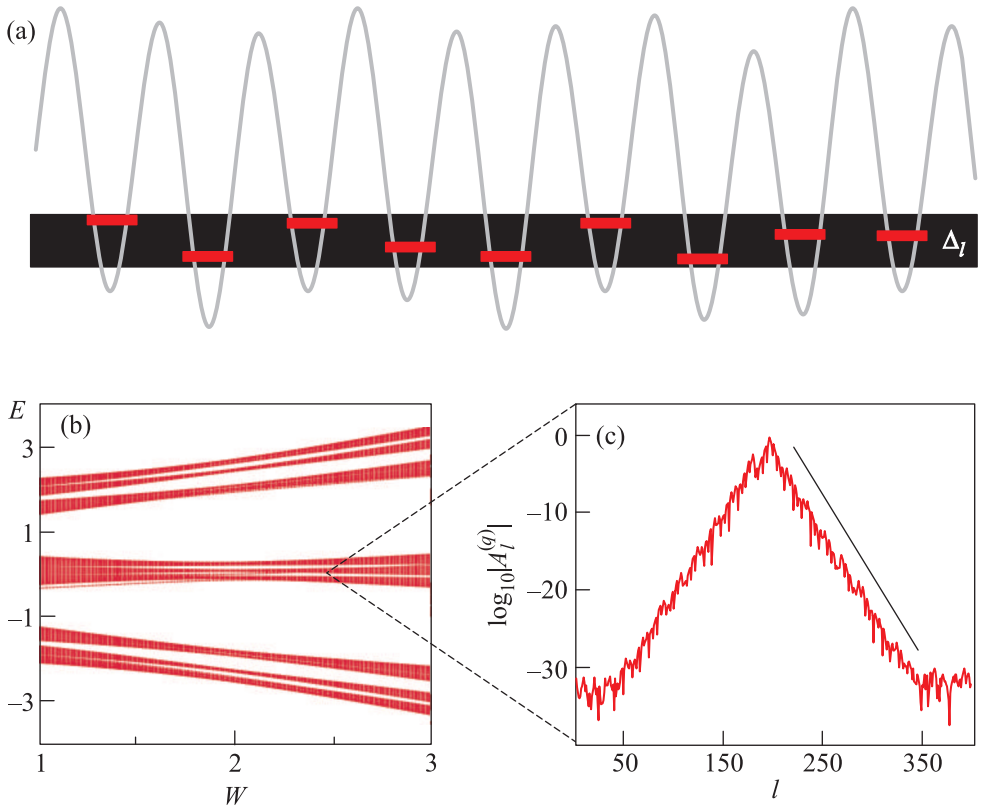

Fig. 1. (Color online) (a) – A sketch of the 1D Aubry–André potential. (b) – Eigenvalues $E = \lambda - 2$ of the linear system, Eq. (3), as a function of the modulation strength W. (c) – Typical exponentially localized eigenstate of in the insulating regime, $W = 2.5$

crete complex Ginzburg–Landau equation. This equation is oftenly used to model transport phenomena in active optical media, non-equilibrium condensate dynamics, and other physical systems [38–40]. We find that the increase of the pumping strength leads to a second-order phase transition from the quiescent state to complex oscillating patterns, both in the metal and insulating regimes. The average oscillation amplitude density scales as $(\alpha - \alpha^*)^\gamma$, $1/2 < \gamma < 1$, approaching the upper limit, characteristic of the disordered lattice, with increasing modulation strength. The density of effectively excited sites displays a diverging derivative near the transition, thus manifesting concurrent delocalization. Strikingly, the transition is accompanied by the onset of global coherence extending even above the metal-insulator transition. Localization Anderson-like attractors are found only in the regime of strong modulations. Finally, we show that multimode oscillations induce dynamical chaos regimes, characterized by the presence of cluster-like synchronization.

We consider a one-dimensional Ginsburg–Landau equation,

$$i\dot{z}_l = \Delta_l z_l + i\left(\alpha - \sigma|z_l|^2\right) z_l + |z_l|^2 z_l - \\ - (1 - i\eta)(z_{l+1} - 2z_l + z_{l-1}), \qquad (1)$$

with incommensurate spatial inhomogeneity $\Delta_l = W\cos(2\pi\alpha l + \beta)$, $\alpha = (\sqrt{5}-1)/2$, where $\beta \in [0, 2\pi]$ is a phase shift. Referring to the Anderson disordered model, we use random disorder, with uncorrelated and uniformly distributed $\Delta_l \in [-W/2, W/2]$. Further on, α is the pumping rate, σ is the nonlinear dissipation coefficient, and η is the strength of dissipative coupling between adjacent sites. Without loss of generality we set conservative nonlinearity and coupling coefficients to one. In numerical studies, finite lattices of size N are used and periodic boundary conditions are imposed, $z_{N+1} = z_1$.

In the linear dissipationless limit, $\alpha = \eta = 0$ and $|z_l|^2 \to 0$, the stationary solutions $z_l = A_l e^{-i\lambda t}$ satisfy

$$\lambda_q A_l^{(q)} = \Delta_l A_l^{(q)} - A_{l+1}^{(q)} + 2A_l^{(q)} - A_{l-1}^{(q)}, \qquad (2)$$

which by $E \equiv \lambda - 2$ reduces to the standard Aubry–Andre eigenvalue problem [7]:

$$E_q A_l^{(q)} = \Delta_l A_l^{(q)} - A_{l+1}^{(q)} - A_{l-1}^{(q)}. \qquad (3)$$

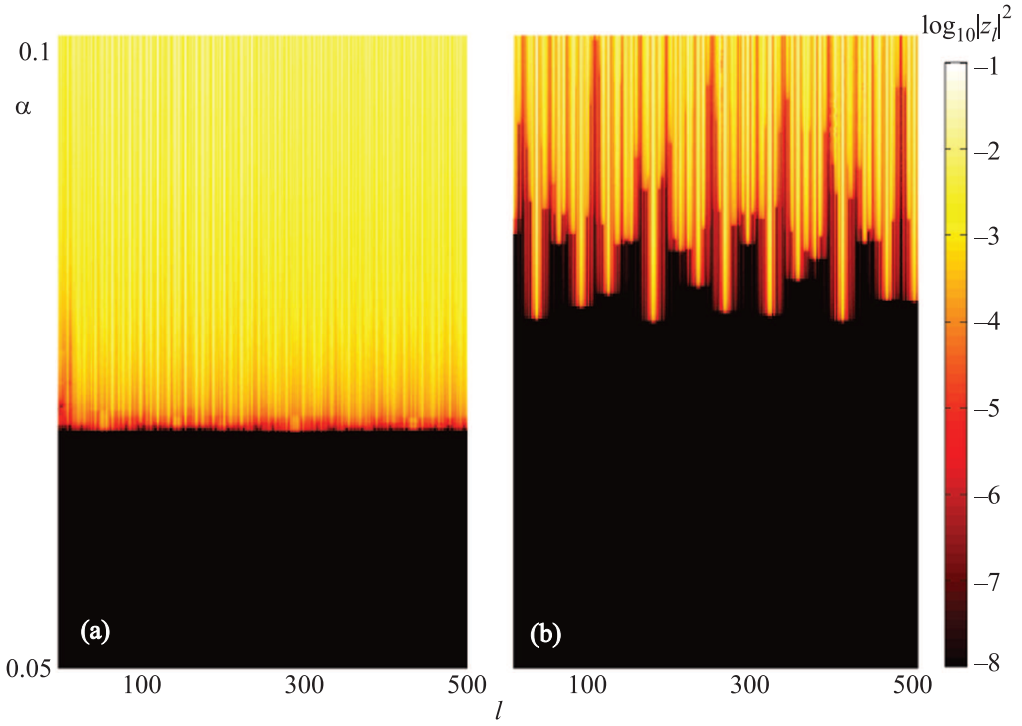

Fig. 2. (Color online) Excitation of oscillations in the quasiperiodic array, Eq. (1), upon the increase of the pumping for weak ($W = 2.02$, a) and strong localization ($W = 2.5$, b). Color encodes time-averaged oscillation amplitudes at lattice sites, $\log_{10}|z_l|^2$, in the attractor regimes as functions of α. The other parameters are $\eta = 0.1,\ N = 1000$

All eigenstates $A_{q,l}$ are extended for $W < 2$ (which is called metallic regime) and exponentially localized for $W > 2$ (insulating state), $|A_l^{(q)}| \sim \exp(-|l - l_q|/\xi)$, with the same localization length $\xi = [\ln(W/2)]^{-1}$, l_q denoting the center of mass (Fig. 1).

For evolution of the net norm $Z = \sum |z_l|^2$ under Eq. (1), we obtain [33]:

$$\dot{Z} = 2\sum \left[(\alpha - \sigma|z_l|^2)|z_l|^2 - \eta|z_{l+1} - z_l|^2\right]. \quad (4)$$

It follows that the zero solution $z_l \equiv 0$ is globally stable for all $\alpha \leq 0$. At the same time, for large enough $\alpha > 0$, low dissipative coupling η, and initially small enough $|z_l|$, the net norm must be growing in time with further saturation. The second term in (4) arises due to nonlinearity, and being of a higher order, is dominated by the third term, arising due to dissipative coupling. Therefore, the homogeneous in-phase solutions $z_{l+1} \approx z_l$ decay slower than the anti-phase ones, $z_{l+1} \approx -z_l$, since they produce a smaller in magnitude negative term (we admit the same $|z_l|$, for comparison).

The linear stability of the zero solution under the action of single-mode perturbations, $z_l(t) = \zeta A_l^{(q)} \exp[(p_q - i\lambda_q)t], \zeta \ll 1$ can be determined from the respective increments p_q. They can be calculated from Eq. (1),

$$p_q = \alpha - \eta \sum \left|A_{l+1}^{(q)} - A_l^{(q)}\right|^2. \quad (5)$$

The necessary stability condition of the zero solution is then $\max p_q < 0$. Note that this quantity depends only on the modulation depth W, lattice phase β, and the ratio between incoherent pumping rate and dissipative coupling, α/η. Moreover, it can be shown that the excitation threshold

$$\frac{\alpha^*}{\eta} = \min_q \frac{\alpha_q^*}{\eta} = \min_q \sum \left|A_{l+1}^{(q)} - A_l^{(q)}\right|^2 \quad (6)$$

is bounded, $0 \leq \alpha^*/\eta \leq 4$, as $\sum_l |A_l^{(q)}|^2 = 1$.

In the vanishing modulation limit $W \to 0$, one recovers the harmonic eigenstates $A_l^{(q)} \sim N^{-1/2}\exp(i\kappa l)$ and spectrum $\lambda_q = 4\sin^2(\kappa/2)$, $\kappa = \pi q/[2(N+1)]$, $q = \overline{1, N}$. In this case the instability threshold (6) is minimized by the lower boundary mode $\lambda_q \to 0$, $\alpha^*/\eta \to 0$ as $N \to \infty$. In the opposite limit $W \gg 1$, deeply in the insulating regime, the modes are essentially single-site localized and $\alpha^*/\eta = \mathcal{O}(1)$. Hence, one can expect that in the metallic phase excitation of some mode (near the lower spectrum boundary) will produce extended oscillation patterns, while in the strongly insulating regime,

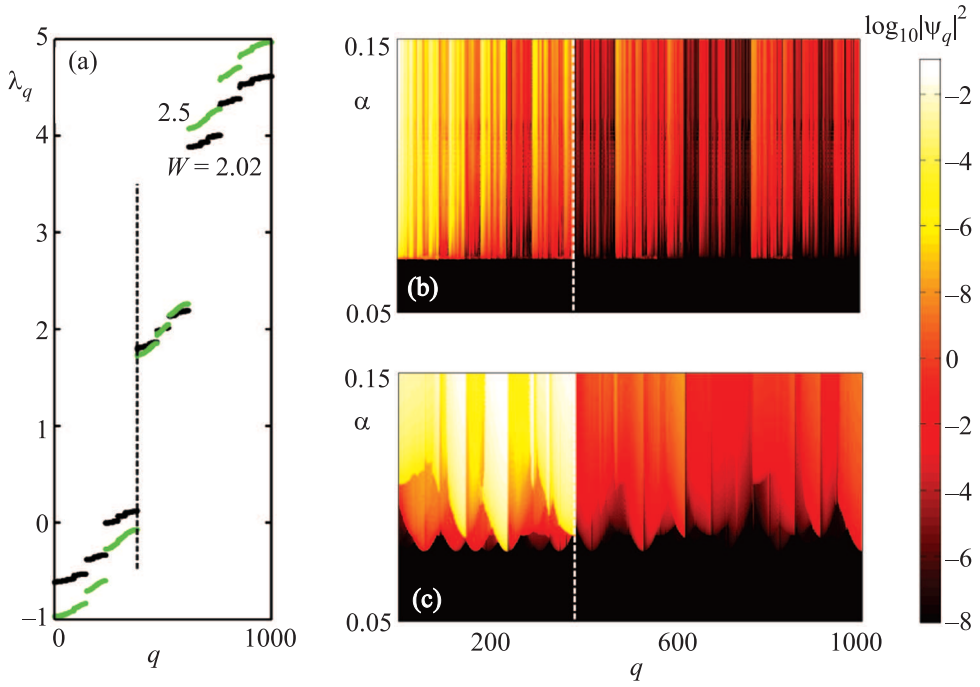

Fig. 3. (Color online) Linear mode space analysis, cf. Fig. 2. (a) – The linear spectrum in the insulating regime of the conservative Aubry–Andre limit, λ_q in the increasing order, displaying three main bands for the given parameters. (b, c) – Color coded mode amplitudes on the attractor, $\log_{10}|\psi_q|^2$ upon the increase of the pumping α for weak ($W = 2.02$, b) and strong localization ($W = 2.5$, c), $N = 1000$. Vertical dashed lines in the panels separate the lower band and indicate its dominating excitation

similar to the case of Anderson disorder [33], one may observe a complex stable pattern consisting of several localized oscillating spots. We called these patterns "localization attractors".

Fig. 2 presents the results of numerical simulations for weak and strong localization, $W = 2.02$ ($\xi \approx 100$) and $W = 2.5$ ($\xi \approx 4$). Profiles for different values of α were obtained as independent *attractor* solutions, by setting system into an initial random low-energy state $|z_l(0)| \ll 1$ and letting it evolve until the corresponding amplitude profile is stabilized. The key distinction of the attractor patterns from the disordered Anderson model [33] is the visually global excitation patterns in the weak localization regime (Fig. 2). At the same time, the pattern of multiple localization peaks away from the metal-insulator transition looks similar to the ones in the Anderson model [33]. Switching to the eigenmode basis, we confirm the conjecture that the modes from the lower band get excited primarily and keep dominating with growing α (Fig. 3).

To study the excitation transition in detail we first compute individual thresholds for the modes (6) and construct their integrated density distribution $F(\alpha^*/\eta)$. (We did not find a substantial size dependence for large enough N.) The results reveal the qualitative difference

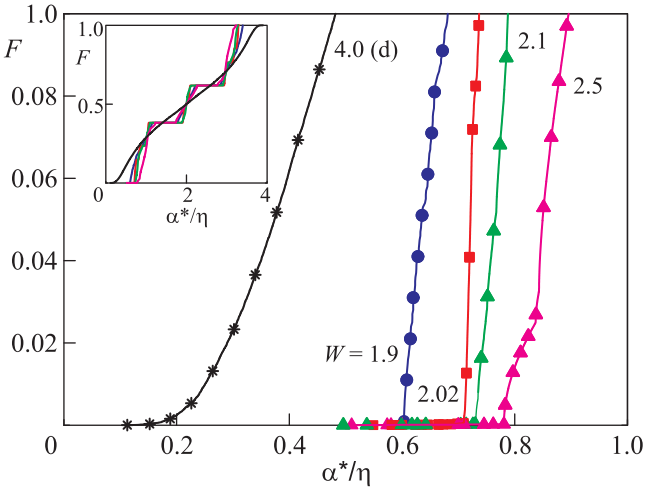

Fig. 4. (Color online) Integrated density of individual mode excitation thresholds $F(\alpha^*/\eta)$ for quasiperiodic arrays with $W = 1.9$ (extended linear states), 2.02, 2.1, and 2.5 (localized states), and for the disordered array with $W = 4$ (d) (localized states). The system size is $N = 5000$. Inset – full-scale plot for the same parameters, colors correspond to the main figure

between quasiperiodic and disordered lattices, that is the vertical (or close to vertical) slope of $F(\alpha^*/\eta)$ about

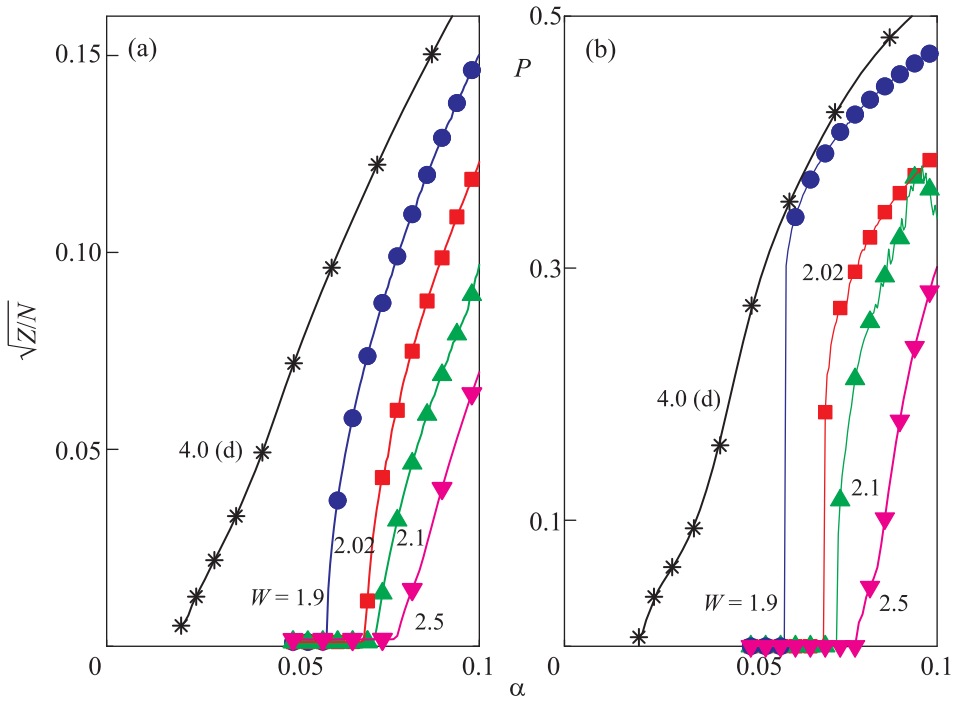

Fig. 5. (Color online) The average amplitude density $\sqrt{Z/N}$ (a) and the participation number P (b) as functions of pumping strength α for quasiperiodic lattices $W = 1.9$ (extended linear states), 2.02, 2.1, 2.5 (localized states), and the disordered array with $W = 4$ (d). The parameters are $\eta = 0.1$ and $N = 1000$

the excitation point (Fig. 4). This property appears to be inherited from the density of states for both models, the Anderson disorder producing Lifshitz tails, absent in the Aubry–Andre case. The further analysis reveals a dramatic effect of such singularity that is collective excitation of modes.

Next we calculate the time-averaged amplitude density, $\sqrt{Z/N}$, and participation number (a quantity conventionally used to estimate the number of effectively excited sites) normalized by the system size,

$$P = \left(\frac{1}{N} \sum |z_l|^4 / Z^2 \right)^{-1}, \qquad (7)$$

as the functions of the pumping strength α (Fig. 5). Notably, passing from extended to localized linear states (at $W = 2$), one would observe that the power-law scaling $\sqrt{Z/N} \propto (\alpha - \alpha^*)^\gamma$ at the excitation threshold point, α^*, changes from $\gamma = 1/2$, as for extended states to $\gamma = 1$, as for Anderson disorder. Moreover, in both metallic and insulating regimes, the participation numbers have diverging slopes at this point $dP/d\alpha \to \infty$, featuring the second order phase transition, in contrast to the disordered case. In other words, quasiperiodic lattices exhibit transition to global oscillations even from the localized regime.

It is instructive to compare the integral distribution of individual mode excitation thresholds, $F(\alpha^*/\eta)$, to the participation number of patterns in the direct space, $P(\alpha)$, keeping in mind that the horizontal axis in Fig. 3 needs to be scaled down by the factor $\eta = 0.1$ to match Fig. 4. Naturally, we observe that the excitation thresholds of the first modes coincide with the rise of $P(\alpha)$. We also notice a good correspondence of the onset of global oscillations, $P \sim 0.25{-}0.5$ for $\alpha \sim 0.07{-}0.1$, cf. also Fig. 3, to the estimated values of pumping, when a large number of modes, $\mathcal{O}(N)$, should become excited, $\alpha \sim 2\eta = 0.1$. In the extended mode regime, $W < 2$, however, this is not the case, since the excitation of a single mode already produces a system-wide oscillation pattern.

We also observe a global coherence in the extended regime, also significantly above the metal-insulator transition. To resolve the phase order we calculate the mean field defined by the expression

$$\rho = \left| \frac{1}{N} \sum z_l \right| / \sqrt{Z/N}. \qquad (8)$$

It typically vanishes in the limit of large systems $N \ll 1$ and uncorrelated phases, $\arg(z_l)$, and takes a finite value $0 < \rho < 1$, if the global order settles.

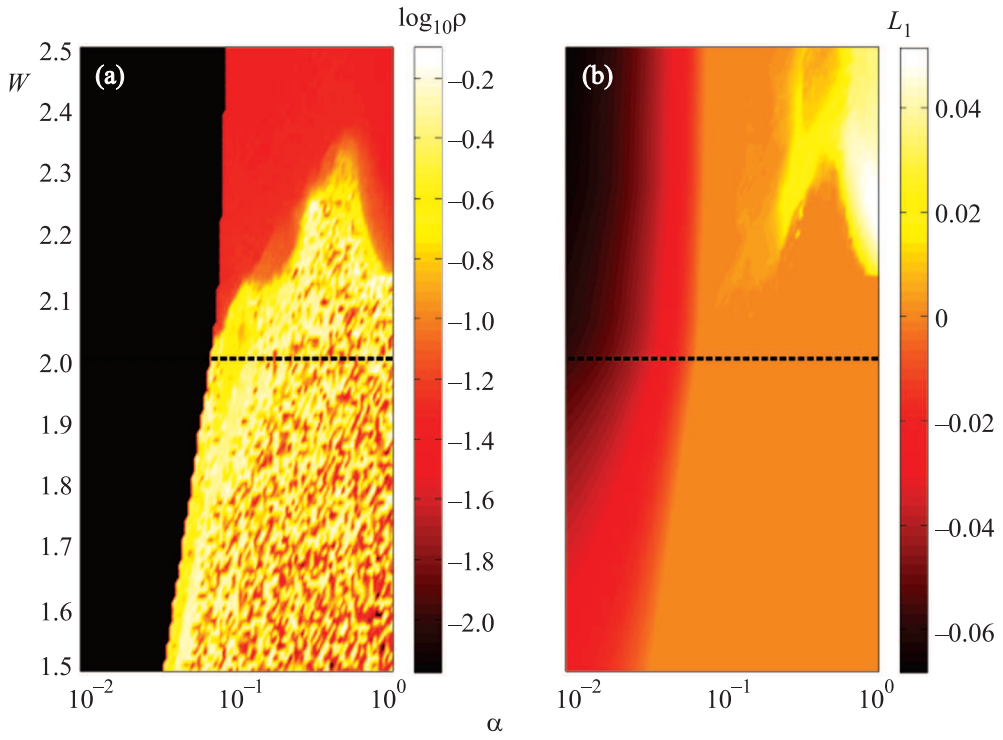

Fig. 6. (Color online) Pumping-modulation depth parameter diagram: color incodes the logarithm of the mean field (a) and largest Lyapunov exponent L_1 (b). Alternating low and high mean spots reveal multistability of coherent and incoherent regimes. Horizontal dashed line at $W = 2$ indicates metal-insulator transition in the Aubry–Andre limit, Eq. (3). The parameters are $\eta = 0.1, N = 1000$

In general, spatial inhomogeneity destroys coherence of phases even if frequencies are near identical, as in the disordered 1D oscillatory arrays [41]. Quasiperiodic arrays present thus an intriguing example of arising nonzero mean field oscillations in the extended and, partly, insulating regime, – at least for sufficiently large although finite systems, see Fig. 6a. As each point on the parameter plane is obtained by evolving randomly chosen initial conditions, alternating spots of high and low ρ indicate multistability of coherent and incoherent states. The border between black and colored parts marks the excitation threshold $\alpha^* = \alpha^*(W)$, with $\alpha^*/\eta \approx 1$ for $W > 2$, corroborating the estimate in the above. The accompanying diagram presents the largest Lyapunov exponent L_1 as a function of the pumping strength and modulation depth (Fig. 6b). Chaos develops in the insulating regime only, and its region has a complex structure with non-monotonous dependence of $L_1(\alpha)$, complementary to that of the synchronized coherent oscillations (cf. Fig. 6a).

As compared to disordered arrays, oscillations in active quasiperiodic systems exhibit qualitatively different features. The interplay of dissipation and energy pumping produces excitation of oscillations at finite pumping strength, corresponding to the linear modes from the lower frequency band. Remarkably, it manifests all the tokens of the second order phase transition and the development of global oscillations not only from the metallic, but also from the weakly insulating conservative states. The global coherence, induced by these oscillations, extends even above the metal-insulator transition. In the strong localization limit, we observe the appearance of localization attractors in form of sparse patterns consisting of several excited Anderson modes. Chaotic synchronized and non-synchronized oscillations gradually appear in the insulating regime as the pumping rate is further increased.

The set of real-life physical systems, where the reported effects can potentially be studied in experiment, includes lattice-like arrays of polariton condensates [25], cavity-QED arrays with the cavities filled up with two-level atoms or qubits [42, 43], systems of coupled Josephson junction [44], and active lasing arrays [19].

T.L. and G.O. acknowledge support of the Russian Science Foundation # 14-12-00811, M.I. and S.D. acknowledge support of Ministry of Education and Science of the Russian Federation (Research Assignment # 1.115.2014/K). M.I. and S.D. conceived the

study, developed the theory, and wrote the manuscript. T.L. and G.O. conducted the numerical experiments and analyzed the results. All authors reviewed the manuscript. Numerical simulations were performed on the Lobachevsky Supercomputer at the Univeristy of Nizhny Novgorod.

1. F. Evers and A. Mirlin, Rev. Mod. Phys. **80** 1355 (2008).
2. *50 Years of Anderson Localization*, ed. by E. Abrahams, World Scientific (2010).
3. F. Bloch, Z. Phys. **52**, 555 (1928).
4. C. Zener, Roy. Soc. London A **137**, 696 (1932).
5. G. H. Wannier, Phys. Rev. **117**, 432 (1960).
6. P. W. Anderson, Phys. Rev. **109**, 1492 (1958).
7. S. Aubry and G. André, Ann. Israel Phys. Soc. **3**, 133 (1980).
8. M. Segev, Y. Silberberg, and D. N. Christodoulides, Nat. Photonics **7**, 197 (2013).
9. H. Hu, A. Strybulevych, J. H. Page, S. E. Skipetrov, and B. A. Van Tiggelen, Nat. Phys. **4**, 945 (2008).
10. J. Billy, V. Josse, Z. Zuo, A. Bernard, B. Hambrecht, P. Lugan, D. Clément, L. Sanchez-Palencia, P. Bouyer, and A. Aspect, Nature **453**, 891 (2008).
11. G. Roati, C. D'Errico, L. Fallani, M. Fattori, C. Fort, M. Zaccanti, G. Modugno, M. Modugno, and M. Inguscio, Nature **453**, 895 (2008).
12. S. S. Kondov, W. R. McGehee, J. J. Zirbel, and B. DeMarco, Science **334**, 66 (2011).
13. F. Jendrzejewski, A. Bernard, K. Muller, P. Cheinet, V. Josse, M. Piraud, L. Pezze, L. Sanchez-Palencia, A. Aspect, and P. Bouyer, Nat. Phys. **8**, 398 (2012).
14. R. Frank, A. Lubatsch, and J. Kroha. Phys. Rev. B **73**, 245107 (2006).
15. T. Eichelkraut, R. Heilmann, S. Weimann, S. Stützer, F. Dreisow, D. N. Christodoulides, S. Nolte, and A. Szameit, Nat. Comm. **4**, 2533 (2013).
16. P. Stano and P. Jacquod, Nat. Photonics **7**, 66 (2013).
17. A. G. Yamilov, R. Sarma, B. Redding, B. Payne, H. Noh, and H. Cao, Phys. Rev. Lett. **112**, 023904 (2014).
18. A. Basiri, Y. Bromberg, A. Yamilov, H. Cao, and T. Kottos, Phys. Rev. A **90**, 043815 (2014).
19. J. Liu, P. D. Garcia, S. Ek, N. Gregersen, T. Suhr, M. Schubert, J. Mork, S. Stobbe, and P. Lodahl, Nat. Nanotechnol. **9**, 285 (2014).
20. Y. V. Fyodorov, JETP Lett. **78**, 250 (2003).
21. R. Nandkishore, S. Gopalakrishnan, and D. A. Huse, Phys. Rev. B **90**, 064203 (2014).
22. R. Balili, V. Hartwell, D. Snoke, L. Pfeiffer, and K. West, Science **316** 1007 (2007).
23. C. W. Lai, N. Y. Kim, S. Utsunomiya, G. Roumpos, H. Deng, M. D. Fraser, T. Byrnes, P. Recher, N. Kumada, T. Fujisawa, and Y. Yamamoto , Nature **450** 526 (2007).
24. D. Tanese, H. Flayac, D. Solnyshkov, A. Amo, A. Lemaitre, E. Galopin, R. Braive, P. Senellart, I. Sagnes, G. Malpuech, and J. Bloch, Nat. Comm. **4**, 1749 (2013).
25. D. Tanese, E. Gurevich, F. Baboux, T. Jacqmin, A. Lemaitre, E. Galopin, I. Sagnes, A. Amo, J. Bloch, and E. Akkermans, Phys. Rev. Lett. **112**, 146404 (2014).
26. T. Kottos and M. Weiss, Phys. Rev. Lett. **93**, 190604 (2004).
27. S. Tietsche and A. Pikovsky, Europhys. Lett. **84**, 10006 (2008).
28. S. Lepri and G. Casati, Phys. Rev. Lett. **106**, 164101 (2011).
29. I. L. Aleiner, B. L. Altshuler, and Y. G. Rubo, Phys. Rev. B **85**, 121301(R) (2012).
30. K. Rayanov, B. L. Altshuler, Y. G. Rubo, and S. Flach, Phys. Rev. Lett. **114**, 193901 (2015).
31. L. Zhang, W. Xie, J. Wang, A. Poddubny, J. Lu, Y. Wang, J. Gu, W. Liu, D. Xu, X. Shen, Y.G. Rubo, B.L. Altshuler, A.V. Kavokin, and Z. Chen, Proc. Nat. Ac. Sci. USA **112**, E1516 (2015).
32. A. A. Tikhomirov, O. I. Kanakov, B. L. Altshuler, and M. V. Ivanchenko, Eur. Phys. J. B **88**, 37 (2015).
33. T. V. Laptyeva, A. A. Tikhomirov, O. I. Kanakov, and M. V. Ivanchenko, Sci. Rep. **5**, 13263 (2015).
34. M. Modugno, New J. Phys. **11**, 033023 (2009).
35. L. Sanchez-Palencia and M. Lewenstein, Nat. Phys. **6**, 87 (2010).
36. B. Deissler, M. Zaccanti, G. Roati, C. DÉrrico, M. Fattori, M. Modugno, G. Modugno, and M. Inguscio, Nat. Phys. **6**, 354 (2010).
37. E. Lucioni, B. Deissler, L. Tanzi, G. Roati, M. Zaccanti, M. Modugno, M. Larcher, F. Dalfovo, M. Inguscio, and G. Modugno, Phys. Rev. Lett. **106**, 230403 (2011).
38. I. S. Aranson and L. Kramer, Rev. Mod. Phys. **74**, 99 (2002).
39. *Dissipative Solitons: From Optics to Biology and Medicine, Lecture Notes in Physics*, ed. by N. Akhmediev and A. Ankiewicz, Springer, Berlin (2008).
40. P. Cristofolini, A. Dreismann, G. Christmann, G. Franchetti, N. G. Berloff, P. Tsotsis, Z. Hatzopoulos, P. G. Savvidis, and J. J. Baumberg, Phys. Rev. Lett. **110**, 186403 (2013).
41. M. G. Rosenblum, A. S. Pikovsky, and J. Kurths, *Synchronization: A Universal Concept in Nonlinear Sciences*, Cambridge University Press, Cambridge, England (2001).
42. E. S. Sedov, A. P. Alodjants, S. M. Arakelian, I. H. Chen, Y. Y. Lin, Y. C. Lai, and R. K. Lee, J. Phys.: Conf. Ser. **393**, 012030 (2012).
43. I.-H. Chen, Y. Y. Lin, Y. C. Lai, E. S. Sedov, A. P. Alodjants, S. M. Arakelian, and R.-K. Lee, Phys. Rev. A **86**, 023829 (2012).
44. D. M. Basko and F. W. J. Hekking, Phys. Rev. B **88**, 094507 (2013).